



## An analytical approach for estimating CO<sub>2</sub> and heat fluxes over the Amazonian region

Xiwu Zhan<sup>a,\*</sup>, Yongkang Xue<sup>b</sup>, G. James Collatz<sup>c</sup>

<sup>a</sup> UMBC-GEST/NASA-GSFC Hydrological Science Branch, Code 974.1, Greenbelt, MD 20771, USA

<sup>b</sup> Department of Geography, UCLA, Los Angeles, CA, USA

<sup>c</sup> Goddard Space Flight Center, Code 923, Greenbelt, MD, USA

Received 17 April 2002; received in revised form 23 October 2002; accepted 20 November 2002

### Abstract

Accurate assessments of the CO<sub>2</sub> fluxes between the terrestrial ecosystems and the atmosphere are pressingly needed for the climate change and carbon cycle studies. The Collatz et al. parameterization of leaf photosynthesis-stomatal conductance has been widely applied in land surface parameterization schemes for simulating the land surface CO<sub>2</sub> fluxes. The study in this paper developed an analytical solution approach for the Collatz et al.'s parameterization for stable solution and computational efficiency. This analytical approach is then applied to the simplified biosphere model (SSiB), enhancing its capability of simulating land surface CO<sub>2</sub> fluxes. The enhanced SSiB model is tested with field observation data sets from two Amazonian field experiments (ABRACOS missions and Manaus Eddy Covariance Study). Simulations of the land surface fluxes of latent heat, sensible heat and soil heat by the enhanced SSiB agree very well with observations with correlation coefficients being larger than 0.80. However, the correlation coefficient for the daily means of CO<sub>2</sub> fluxes is only 0.42 for the Manaus data set. A day-time “square wave” in the simulated CO<sub>2</sub> flux diurnal curves is found. The discrepancies between simulation and observation were found to be the results of incorrect parameter setup or improper leaf to canopy scaling strategy. A modification to the scaling strategy improves significantly the accuracy of the photosynthesis-stomatal conductance model.

© 2002 Published by Elsevier Science B.V.

**Keywords:** Photosynthesis; Stomatal conductance; CO<sub>2</sub>; Energy balance; Simplified biosphere model (SSiB); Analytical solution; ABRACOS; LBA

### 1. Introduction

Since the late 1970s, numerical modeling experiments using the coupled atmospheric and land surface models have been carried out to explore the relationship between land surface characteristics and the global as well as regional climate. These studies have shown that the changes in land surface characteristics,

such as albedo, surface roughness length, vegetation properties, and soil properties, could substantially alter terrestrial hydrologic system at global and regional scales (see reviews by Sellers et al., 1997; Kabat and Claussen, 2002). In these studies, biophysical models with different complexity have been developed. The project for intercomparison of land-surface parameterization scheme (PILPS, Henderson-Seller et al., 1993, 1995) has also been carried out to evaluate and improve the land surface parameterizations, and, therefore, to enhance the models' ability predicting the water cycle. In these models, however, empirical work

\* Corresponding author. Tel.: +1-301-286-3885;

fax: +1-603-806-8375.

E-mail address: xzhan@hab.gsfc.nasa.gov (X. Zhan).

45 had correlated stomatal conductance to the environ-  
46 mental conditions independent from any consideration  
47 of photosynthesis. By the late 1980s, scientific inter-  
48 est on global change, particularly on the “greenhouse  
49 effect” had promoted the development of more com-  
50 plete models, which directly couple water and carbon  
51 cycle processes (Sellers et al., 1997).

52 Increase in greenhouse gases, in particular CO<sub>2</sub>,  
53 has great impacts on global climate change. The po-  
54 tential importance of land carbon cycle to the global  
55 climate was suggested in Cox et al. (2000) who per-  
56 formed future climate simulations with interactive  
57 vegetation and ocean carbon cycles. Their simula-  
58 tions produced significant climate warming caused by  
59 climate-induced loss of Amazonian rainforests. Re-  
60 cent studies have shown that terrestrial ecosystems,  
61 especially tropical rain forest, may be an important  
62 sink of atmospheric CO<sub>2</sub> (Tian et al., 2000; Schimel  
63 et al., 2001). Regional studies based on in situ mea-  
64 surements are consistent with carbon sinks associated  
65 with tropical forests (Phillips et al., 1998). The Ama-  
66 zon region contains the largest area of tropical forest  
67 on Earth. Over the past 25 years, rapid development  
68 has led to the destruction of over 500,000 km<sup>2</sup> of  
69 forest in Brazil (Houghton et al., 2000), producing a  
70 large source for atmospheric CO<sub>2</sub>. Study has found  
71 that the Amazonian region acted as a net source for  
72 carbon in a range of 0.2–1.2 Pg year<sup>-1</sup> from 1992  
73 to 1993 mainly because of the deforestation (Keller  
74 et al., 2001). Since emissions from land clearing in  
75 the tropics are thought to be large, there must be off-  
76 setting sinks to balance these emissions. All of these  
77 indicate a pressing need for accurate assessments of  
78 the CO<sub>2</sub> fluxes between the terrestrial ecosystems and  
79 the atmosphere.

80 Two efforts are required to address this need: one  
81 is the observation of CO<sub>2</sub> fluxes between a terrestrial  
82 ecosystem and the atmosphere in field for ground  
83 truth; and the other is the development and validation  
84 of models to understand the observed evidence and to  
85 extrapolate the modeling results to the other regions.  
86 The first effort has been made in many large-scale  
87 field experiments, one of which is the Large-Scale  
88 Biosphere-Atmosphere Experiment in Amazonia  
89 (LBA, Keller et al., 1997). A number of other field  
90 data sets have been collected in this region for analy-  
91 ses and model validation. In the study of this paper,  
92 the data from Anglo-Brazilian Amazonian Climate

Observation Study (ABRACOS, Gash et al., 1996) 93  
and another measurement in central Amazonian rain 94  
forest (Malhi et al., 1998) are used. 95

96 In addition to field measurement, great deal of 96  
effort has been carried out to develop plant photo- 97  
synthesis models since 1970s (Thornley and Johnson, 98  
1990) and has gained more attention from the ecolog- 99  
ical science (Jorgensen, 1997) and climate modeling 100  
communities (Sellers et al., 1992). This model de- 101  
velopment effort is still going on (Boonen et al., 102  
2002). Collatz et al. (1991, 1992) combined the bio- 103  
chemical photosynthesis model in Farquhar et al. 104  
(1980) with the semi-empirical stomatal conductance 105  
model of Ball (1988) to estimate stomatal conduc- 106  
tance and photosynthesis rate of leaves simultane- 107  
ously. We will refer Collatz et al. parameterization of 108  
leaf photosynthesis-stomatal conductance as Collatz 109  
et al. model in this paper. Taking advantages of its 110  
strong physical and biochemical bases, Sellers et al. 111  
(1996a) adapted this coupled photosynthesis-stomatal 112  
conductance model in the revised Simple Biosphere 113  
model (SSiB\_2) for simulating land surface energy 114  
and CO<sub>2</sub> fluxes by scaling up leaf responses to the 115  
canopy level. The SSiB\_2 model has been applied 116  
in global climate and carbon cycle studies (Sellers 117  
et al., 1996a,b; Sellers et al., 1997; Denning et al., 118  
1996a,b). However, the iterative solution used in the 119  
photosynthesis-stomatal conductance model is compu- 120  
tationally expensive and also may become numerically 121  
unstable under certain environmental conditions 122  
(Baldocchi, 1994). Proper procedure must be taken to 123  
avoid such circumstances. In contrast, an analytical 124  
solution for the coupled leaf photosynthesis-stomatal 125  
conductance model can avoid these problems. 126

127 Baldocchi (1994) made an early attempt to derive an 127  
analytical solution of the leaf photosynthesis equations 128  
in Farquhar et al. (1980) and stomatal conductance in 129  
Ball (1988). The equations used in Baldocchi (1994) 130  
are similar to those in Collatz et al. (1991), but they dif- 131  
fer from those in Sellers et al. (1996a), which includes 132  
scaling from leaf to vegetation canopies. In addition, 133  
the version of the Collatz et al.’ model in Sellers et al. 134  
(1996a) considers broader environmental conditions. 135  
For example, the photosynthesis equations of Collatz’ 136  
coupled model in Sellers et al. (1996a) takes accounts 137  
of three photosynthetic limitations rather than the two 138  
photosynthetic limitations considered by Baldocchi 139  
(1994). Thus, an analytical approach for the Collatz’ 140

141 coupled model in Sellers et al. (1996a) should be dif-  
 142 ferent from those in Baldocchi (1994). Because of the  
 143 wide applications of the Collatz et al. model (Bonan,  
 144 1995; Sellers et al., 1996a,b; Denning et al., 1996a,b;  
 145 Chen et al., 1999), deriving its analytical solutions of  
 146 the more complex form should provide a useful ap-  
 147 proach for the global climate and carbon cycling stud-  
 148 ies.

149 The simplified biosphere model (SSiB) of Xue et al.  
 150 (1991) has been evaluated by observational data from  
 151 different vegetation types and different geographical  
 152 location, and has been broadly used in global and re-  
 153 gional climate studies, including the LBA (for exam-  
 154 ple, Xue et al., 1996a; Chou et al., 2002). However,  
 155 the current version of SSiB uses Jarvis' empirical ap-  
 156 proach (Jarvis, 1976) for the formulation of stomatal  
 157 conductance. It does not consider the photosynthetic  
 158 activities of land surface vegetation and is thus unable  
 159 to estimate land surface CO<sub>2</sub> fluxes for carbon cycling  
 160 studies. In this paper, we attempt to enhance the SSiB  
 161 model by deriving an analytical solution from Col-  
 162 latz et al. model and to apply it to SSiB. Replacing  
 163 the empirical stomatal resistance submodel in SSiB  
 164 with Collatz et al. model, the SSiB model is then re-  
 165 vised to have the CO<sub>2</sub> flux simulation capability. To  
 166 test this extended capability of the SSiB model as a  
 167 part of our effort within the LBA frame, we ran the  
 168 model with the observational data from two large-scale  
 169 field experiments held in Amazonian tropical forests.  
 170 The output from the model is analyzed against their  
 171 corresponding field observations. Discrepancies be-  
 172 tween simulation and observation were found as a re-  
 173 sult of incorrect parameter setup or improper leaf to  
 174 canopy scaling strategy. A modification to the scal-  
 175 ing strategy improves significantly the accuracy of the  
 176 photosynthesis-stomatal conductance model. Finally,  
 177 further improvement of the revised SSiB model is dis-  
 178 cussed. It is important to note that the net CO<sub>2</sub> flux  
 179 from the land surface is a function of both photosyn-  
 180 thetic uptake and respiratory release by plants and de-  
 181 composition. The latter is not addressed here and will  
 182 be the focus of future updates to the model.

183 **2. Collatz et al. model**

184 The equations and parameterizations of plant pho-  
 185 tosynthesis  $A_n$  and stomatal conductance  $g_s$  developed

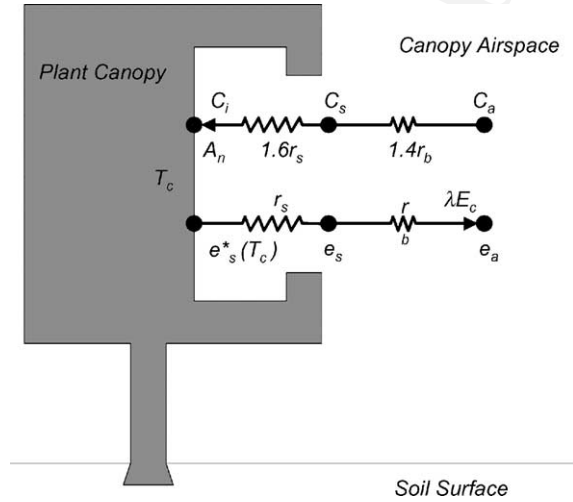


Fig. 1. Schematic diagram of Collatz' coupled photosynthesis-stomatal conductance model (canopy version in Sellers et al., 1996a). See Appendix A for symbol definition.

186 by Collatz et al. (1991) for C<sub>3</sub> plants and by Collatz  
 187 et al. (1992) for C<sub>4</sub> plants are scaled up from leaf to  
 188 canopy level in Sellers et al. (1996a). These equations  
 189 have sound physiological bases and thorough descrip-  
 190 tions to the interactive effects of environmental fac-  
 191 tors and stomatal control of plant photosynthesis and  
 192 transpiration. In the leaf to canopy scaling-up strat-  
 193 egy used in Sellers et al. (1996a), a plant canopy is  
 194 simplified as a “big leaf”. Fig. 1 is the schematic di-  
 195 agram showing the exchanges of sensible heat, latent  
 196 heat and CO<sub>2</sub> between atmosphere and the canopy in  
 197 Collatz et al. model (1991, 1992). The formations of  
 198 Sellers et al. (1996a) can be summarized in the fol-  
 199 lowing five equations:

$$A_n = \frac{g_b}{1.4} \frac{C_a - C_s}{p} \quad (1) \quad 200$$

$$A_n = \frac{g_s}{1.6} \frac{C_s - C_i}{p} \quad (2) \quad 201$$

$$g_s = m \frac{pA_n e_s}{C_s e^*(T_c)} + bF \quad (3) \quad 202$$

$$A_n = \min(W_c, W_e, W_s) - R_d \quad (4) \quad 203$$

$$g_s(e^*(T_c) - e_s) = g_b(e_s - e_a) \quad (5) \quad 204$$

205 The symbols in these equations are listed in Appendix  
 206 A. Eq. (1) describes CO<sub>2</sub> transfer rate from canopy

airspace to leaf surface. Eq. (2) estimates CO<sub>2</sub> transfer rate from leaf surface to inside the stomata. Eq. (3) shows the relationship between stomatal conductance and photosynthesis at canopy scale based on Ball's (1988) stomatal conductance model. Eq. (4) is the leaf biochemical model that includes the leaf to canopy scaling approach of Sellers et al. (1992). Eq. (5) is the conservation equation for water transfer from inside stomata through stomata to the canopy airspace. The three limitations ( $W_c$ ,  $W_e$  and  $W_s$ ) of photosynthetic rate in Eq. (4) are computed as follows for  $C_3$  plants:

$$W_c = V_{\max} \frac{C_i - \Gamma_*}{C_i + K_c(1 + O_i/K_o)} \Pi \quad (6)$$

$$W_e = \text{PAR}(1 - \omega\Pi)\varepsilon_3 \frac{C_i - \Gamma_*}{C_i + 2\Gamma_*} \Pi \left( \frac{\overline{G(\mu)}}{\mu} \right) \quad (7)$$

$$W_s = 0.5V_{\max}\Pi \quad (8)$$

For  $C_4$  plants, they are calculated with the following equations:

$$W_c = V_{\max}\Pi \quad (9)$$

$$W_e = \text{PAR}(1 - \omega\Pi)\varepsilon_4\Pi \left( \frac{\overline{G(\mu)}}{\mu} \right) \quad (10)$$

$$W_s = V_{\max}2 \times 10^4 \frac{C_i}{p} \quad (11)$$

In these equations, the leaf to canopy scaling factor:

$$\Pi = \frac{VN(1 - e^{-\bar{k}F/VN})}{\bar{k}} \quad (12)$$

The inputs needed by these equations include PAR,  $T_a$ ,  $T_c$ ,  $e_a$ ,  $C_a$  and  $g_b$ . The unknown variables are  $A_n$ ,  $g_s$ ,  $C_i$ ,  $C_s$  and  $e_s$  (see Appendix A for symbol definitions).

### 3. Semi-analytical solution approach

Since Eqs. (1)–(5) are high-order non-linear functions, full analytical solutions cannot be obtained. Collatz et al. (1991, 1992) and Sellers et al. (1996a) use iterations to obtain numerical solutions. In this study, a semi-analytical solution procedure is developed. To simplify the solution, we first set the value of  $e_s$  to be the average of  $e_a$  and  $e^*(T_c)$ . Therefore,

only Eqs. (1)–(4) are used to derive analytical solutions. We further rewrite Eq. (4) in a general form as follows:

$$A_n = A_1 \frac{C_i - A_2}{A_3 C_i + A_4} + A_5 \quad (13)$$

The expression for each  $A_i$  ( $i = 1, 2, 3, 4, 5$ ) for  $C_3$  and  $C_4$  plants is listed in Table 1.

If  $A_1 \neq 0$  and  $A_3 \neq 0$  in Eq. (13), a cubic equation of  $C_i$  can be derived from Eqs. (1)–(3) and (13):

$$AC_i^3 + BC_i^2 + CC_i + D = 0 \quad (14)$$

If  $A_1 \neq 0$  and  $A_3 = 0$  in Eq. (13), a quadratic equation would be obtained:

$$a_c C_i^2 + b_c C_i + c_c = 0 \quad (15)$$

A detailed derivation and the definitions of the coefficients in Eqs. (14) and (15) are presented in Appendix B.

With the valid solution of  $C_i$  obtained from the above procedure, we use Eq. (13) to computer  $A_n$  if  $A_3 \neq 0$ . Otherwise,

$$A_n = A_1 C_i + A_5 \quad (16)$$

From the value of  $A_n$ , we can inverse Eq. (1) to obtain the value of  $C_s$  and finally the value of  $g_s$  can be obtained from Eq. (3).

Fig. 2 is a flow chart of the above semi-analytical solution procedure. It starts from estimating the “leaf” surface water vapor pressure with the average of the canopy space water vapor pressure and the water vapor pressure insides the stomata. For any set of environmental conditions, the coefficients of Eq. (14) can be computed with the equations in Appendix B. Then an analytical solution of  $C_i$  can be obtained by analytically solving the cubic equation. Once the value of  $C_i$  corresponding to the set of the environmental conditions is obtained, the values of  $A_n$ ,  $g_s$ ,  $C_s$  and a new  $e_s$  can be obtained. The new  $e_s$  value is normally very close to its previous value. If not, the coefficients of Eq. (14) can be re-computed with the new  $e_s$  value and the steps to solve the cubic equation and to compute the values of  $A_n$ ,  $g_s$ ,  $C_s$  and  $e_s$  will be repeated. This procedure has two important aspects: (1) with the analytic approach, the physically and biologically unrealistic solutions are avoided. Under any specific environmental conditions, whether reasonable solutions of the model can be obtained depends on whether the

Table 1  
Expressions of the variables  $A_i$  ( $i = 1, 2, 3, 4, 5$ ) in Eq. (13)

Plant type	Photosynthetic limitation	$A_1$	$A_2$	$A_3$	$A_4$	$A_5$
C <sub>3</sub>	$W_c$	$V_{\max} \Pi$	$\Gamma_*$	1	$K_c(1 + O_i/K_o)$	$-R_d$
	$W_e$	$\text{PAR}(1 - \omega_{\Pi})\varepsilon_3 \Pi (\overline{G(\mu)})/\mu$	$\Gamma_*$	1	$2\Gamma_*$	$-R_d$
	$W_s$	$0.5V_{\max} \Pi$	0	1	0	$-R_d$
C <sub>4</sub>	$W_c$	$V_{\max} \Pi$	0	1	0	$-R_d$
	$W_e$	$\text{PAR}(1 - \omega_{\Pi})\varepsilon_4 \Pi (\overline{G(\mu)})/\mu$	0	1	0	$-R_d$
	$W_s$	$2 \times 10^4 (V_{\max}/p) \Pi$	0	0	1	$-R_d$

283 cubic equation of  $C_i$  has a realistic solution. We have  
 284 tested the above method under a range of environmental  
 285 conditions, and have not found any case with no  
 286 valid solution. (2) The initial value of  $e_s$  is very close  
 287 to its solution when wind speed is not very large which  
 288 is true for most leaves within a canopy, so that ex-  
 289 cluding  $e_s$  in the analytical solution procedure makes  
 290 the derivation simple. Although we list iteration for  $e_s$   
 291 in Fig. 2, in most cases, no iteration is needed when  
 292 the initial conditions of  $e_s$  are selected as described  
 293 above.

294 Fig. 3 demonstrates the results from the above semi-  
 295 analytical solution method compared with the re-  
 296 sults from the iterative numerical solution method  
 297 for a set of typical environmental conditions listed  
 298 in Table 2. Sensitive parameters are also listed in  
 299 Table 2. Other parameter values are adopted from  
 300 Sellers et al. (1996a). The results are almost identi-  
 301 cal in most cases except that the numerical solution

Table 2  
The typical environmental conditions and model parameters for the plots in Fig. 3

Canopy leaf area index LAI	3.0
Above canopy CO <sub>2</sub> concentration $C_a$	34 Pa
Above canopy air temperature $T_a$	25 °C
Above canopy vapor pressure $e_a$	2000 Pa
“Leaf” boundary layer resistance $r_b$	50 s m <sup>-1</sup>
Rubisco maximum catalytic capacity $V_{\max}$	60 μmol m <sup>-2</sup> s <sup>-1</sup>
PAR extinction coefficient $\kappa$	0.45
Time-mean projection of leaves $[G(\mu)/\mu]$	1.0
Photosynthesis optimal temperature top	30 °C
Photosynthesis minimum temperature $T_{low}$	15 °C
Photosynthesis maximum temperature $T_{high}$	45 °C

method may become unstable when the value of PAR 302  
 becomes higher than 400 (W m<sup>-2</sup>). This confirms the 303  
 potential instability problem in iterations as claimed 304  
 in Baldocchi (1994). 305

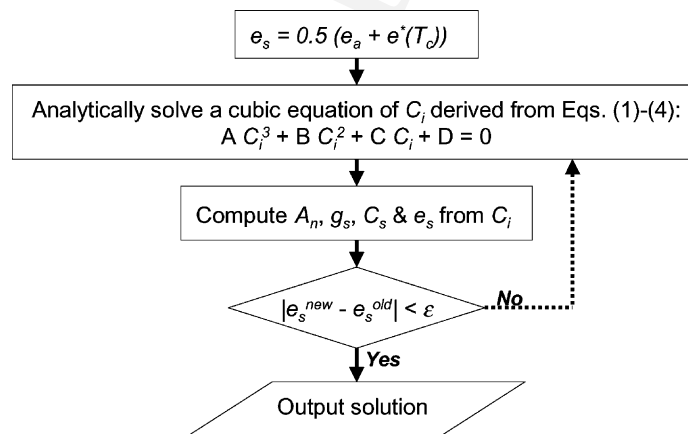


Fig. 2. The semi-analytical solution procedure for the Collatz et al.  $A_n-r_s$  coupled model.

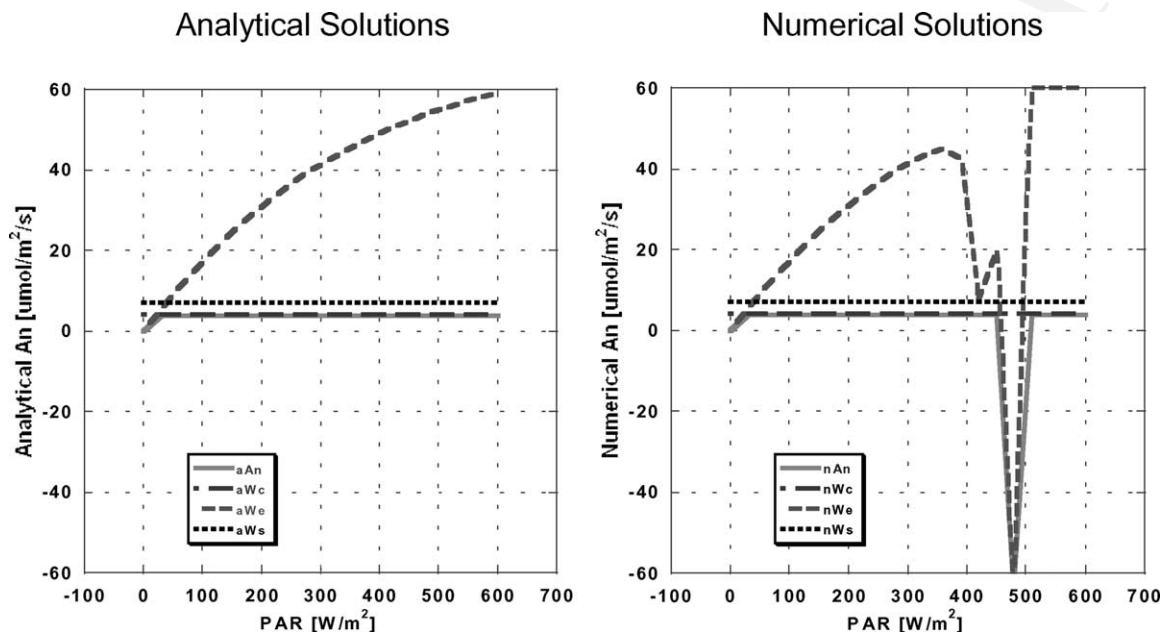


Fig. 3. Comparison between the analytical and numerical solution methods for the Collatz et al.  $A_n-r_s$  coupled model. The symbols  $aA_n$ ,  $aW_c$ ,  $aW_e$ ,  $aW_s$  represent results from the analytical solution approach. The symbols  $nA_n$ ,  $nW_c$ ,  $nW_e$ ,  $nW_s$  are the results from the numerical iteration method.

306 **4. Implementing Collatz et al. model in the**  
 307 **simplified biosphere model (SSiB)**

308 Stomatas on plant leaves control both water vapor  
 309 transfer from inside to outside and  $CO_2$  transfer from  
 310 outside to inside as indicated in Fig. 1. The original  
 311 SSiB model (Xue et al., 1996a,b) simulates only the  
 312 water vapor transfer by using the Jarvis' empirical ap-  
 313 proach (Jarvis, 1976) to compute the stomatal resi-  
 314 stance  $r_c$  to water vapor transfer. With the reasons stated  
 315 previously, we enhance the SSiB model with the  $CO_2$   
 316 simulation capability by replacing the submodel of  
 317 stomatal resistance in the original SSiB with the Col-  
 318 latz et al. model introduced in the previous sections.

319 To compute the canopy resistance (the inverse of  
 320 canopy stomatal conductance) with the photosyn-  
 321 thesis-stomatal conductance model (Eqs. (1)–(5)), one  
 322 needs to know the canopy airspace  $CO_2$  concentration  
 323  $C_a$ . The value of  $C_a$  needs to be specified first, which  
 324 is the product of the balance of  $CO_2$  fluxes into and  
 325 out of the canopy airspace. For a typical day-time,  
 326 the influxes include the  $CO_2$  transfer from the at-  
 327 mosphere and from the soil surface into the canopy

airspace, namely  $F_{ca}$  and  $F_{cs}$ . The sink of the canopy  
 328 airspace  $CO_2$  is the canopy photosynthesis  $A_n$ . If  $F_{cs}$   
 329 and the  $CO_2$  concentration of the atmosphere above  
 330 the canopy,  $C_m$ , are known, then we have  
 331

$$C_a = C_m - pr_a(A_n - F_{cs}) \quad (17) \quad 332$$

because  
 333

$$F_{ca} = \frac{C_m - C_a}{pr_a} = A_n - F_{cs}. \quad (18) \quad 334$$

335 Eq. (18) can be used to simulate the  $CO_2$  flux above  
 336 a plant canopy. The soil respiration term  $F_{cs}$  in the  
 337 above equations will be the focus of future updates of  
 338 the model. In this paper, it is setup to be a constant  
 339 (e.g.  $F_{cs} = 4.0 \mu mol m^{-2} s^{-1}$  for the Manaus data set  
 340 described in Section 6.2).

341 Soil moisture is an important factor influencing the  
 342 carbon flux. In SSiB, the equation of the adjustment  
 343 factor  $f(\psi)$  of the stomatal conductance  $g_s$  for soil  
 344 moisture limitation is

$$f(\psi) = 1 - \exp\{-C_2[C_1 - \ln(-\psi)]\} \quad (19) \quad 345$$

where  $\psi$  is the soil water potential.  $C_2$  depends on the vegetation type, and  $C_1$  is a constant obtained using the wilting point. The stomates completely close at the wilting point in the model.  $C_2$  is a slope factor. A large  $C_2$  means that the  $f(\psi)$  changes from 0 to 1 very fast when soil water content varies from wilting point to the point stomates start to close. This approach differs from that of Sellers et al. (1996a,b) who apply water stress scaling to the maximum photosynthetic capacity ( $V_{\max}$ ) rather than the stomatal conductance directly. Note that in Table 1 of Xue et al. (1991) the values of  $C_1$  and  $C_2$  should be interchanged.

### 5. Scaling up the Collatz et al. model from leaf to canopy

Fig. 3 indicates that canopy net photosynthesis rate gets saturated when photosynthetically active radiation PAR is greater than about 50 ( $\text{W m}^{-2}$ ). According to field measurements introduced in Section 6 and documentations in the literature (e.g. Thornley and Johnson, 1990), this saturation PAR level for most leaves is greater than 200 ( $\text{W m}^{-2}$ ). One of the causes may be that implementation of the Collatz et al. model in the SSiB\_2 model (Sellers et al., 1996a,b) assumes equal acceptance of PAR by all leaves within a canopy when the equations are integrated for all leaves in the canopy. In reality, only sunlit leaves in plant canopy receive direct PAR while shaded leaves receive diffusive PAR only. To consider this fact, we implement the Collatz et al. model for sunlit leaves and shaded leaves separately while the equation set (Eqs. (1)–(12)) and the analytical solution approach introduced previously are kept the same.

Instead of using the total PAR for the Collatz et al. model, we separate PAR to direct radiation  $\text{PAR}_{\text{dr}}$  and diffusive radiation  $\text{PAR}_{\text{df}}$ . According to Norman (1982), if the PAR measurement above the canopy is  $\text{PAR}_0$  and the fraction of diffusive PAR is  $f_d$ , then

$$\text{PAR}_{\text{df}} = f_d \text{PAR}_0 \exp(-0.5F^{0.7}) + 0.07(1 - f_d) \text{PAR}_0 (1.1 - 0.1F) e^{-\sin \theta_s} \quad (20)$$

$$\text{PAR}_{\text{dr}} = \frac{(1 - f_d) \text{PAR}_0 \cos \theta_{\text{ls}}}{\sin \theta_s} \quad (21)$$

where  $\theta_s$  is elevation angle of the sun and calculated from the time of day, the day of year and the latitude of observational site with the equation used in Campbell (1977, p. 55). The  $\theta_{\text{ls}}$  is the mean angle between the leaf normal and the sunlight. We select  $\theta_{\text{ls}} = 60^\circ$  for a canopy with spherical leaf angle distribution (Norman, 1982). Accordingly, the PAR received by the sunlit leaves  $\text{PAR}_{\text{slt}} = \text{PAR}_{\text{dr}} = \text{PAR}_{\text{df}}$  while the PAR received by the shaded leaves  $\text{PAR}_{\text{shd}} = \text{PAR}_{\text{df}}$ .

Assuming random leaf positioning and spherical leaf angle distribution, the sunlit leaf area index  $F_{\text{slt}}$  as

$$F_{\text{slt}} = 2[1 - \exp(-0.5F/\sin \theta_s)] \sin \theta_s \quad (22)$$

the shaded leaf area index  $F_{\text{shd}} = F - F_{\text{slt}}$ .

Using  $\text{PAR}_{\text{slt}}$  to run the analytical solution procedure for the Collatz et al. model introduced previously for a unit sunlit leaf (leaf area index = 1.0), one obtains the net photosynthesis rate  $A_{\text{nslt}}$  and stomatal conductance  $g_{\text{slt}}$ . Similarly using  $\text{PAR}_{\text{shd}}$  for a unit shaded leaf, one obtains  $A_{\text{nshd}}$  and  $g_{\text{shd}}$ . The canopy total net photosynthetic rate  $A_n$  and stomatal conductance are then computed as

$$A_n = A_{\text{nslt}} F_{\text{slt}} + A_{\text{nshd}} F_{\text{shd}} \quad (23)$$

$$g_c = \frac{1}{(F_{\text{slt}}/g_{\text{slt}}) + (F_{\text{shd}}/g_{\text{shd}})} \quad (24)$$

By this point, we have introduced three different versions of implementing the Collatz et al. model of plant photosynthesis and stomatal conductance: (1) the original implementation in SSiB\_2 using iteration solution method; (2) a modified version using analytical solution method; and (3) another modified version using both the analytical solution method and the sunlit–shaded leaf separation scaling method. For this study of enhancing the SSiB for carbon simulation, we use field measurements to evaluate the following three versions of SSiB: (1) the original SSiB model using Jarvis' stomatal model (for convenience we will refer this version as SSiB\_0); (2) the SSiB model using the Collatz et al. model in Sellers et al. (1996a) modified with the analytical solution method (referred to as SSiB\_1); and (3) the SSiB model using the Collatz et al. model modified with the analytical solution method and the sunlit–shaded leaf separation scaling method (referred to as SSiB\_2).

## 431 6. Field measurement data sets for model 432 evaluation

433 Three data sets from two field experiments are used  
434 to evaluate the enhanced SSiB model. The two field  
435 experiments are the ABRACOS field experiment and  
436 the Manaus Eddy Covariance Study.

### 437 6.1. ABRACOS field experiment (1990 and 1991)

438 The ABRACOS is a comprehensive observational  
439 study of land surface–atmosphere interactions in  
440 large-scale clearings caused by tropical deforestation  
441 (Shuttleworth et al., 1991). The main objective of  
442 ABRACOS was to provide comparative data from ad-  
443 jacent forested and cleared areas, and to provide rep-  
444 resentative parameters and data from clearings for  
445 GCM studies. The data used in this study were collec-  
446 ted during the first two experimental seasons of  
447 ABRACOS at the Fazenda Dimona ranch site  
448 ( $02^{\circ}19'S$ ,  $60^{\circ}19'W$ ), 100 km north of Manaus in  
449 central Amazonia. Mission 1 was conducted from  
450 4 October to 2 November 1990 and Mission 2 was  
451 conducted from 29 June to 10 September 1991. Veg-  
452 etation at the experiment site is mainly  $C_4$  grass.  
453 Further details of the ranch and the experimental site  
454 are described by Wright et al. (1992), McWilliams  
455 et al. (1993), and Bastable et al. (1993).

456 The ABRACOS Mission 1 (M1) and Mission 2  
457 (M2) data sets include incoming and reflected radi-  
458 ation of wavelength 0.3–3.0  $\mu\text{m}$ , global radiation, soil  
459 heat flux, ambient air and wet-bulb temperatures, soil  
460 temperature, precipitation, and wind speed and di-  
461 rection. Manufacturer supplied calibrations were used  
462 for all the radiation instruments. The thermometers  
463 were calibrated against a standard and are accurate  
464 to within  $\pm 0.1$  K. The data were recorded using solid  
465 state recorder, which sampled every 10 s.

466 Three measurement systems, including a Campbell  
467 Scientific Ltd. (UK) Bowen-ratio system, the Mk 2  
468 ‘Hydra’ Eddy correlation device, and a logarithmic  
469 wind and scalar profile measurement rig were used to  
470 estimate fluxes of water vapor and sensible heat. There  
471 was excellent agreement between the three measure-  
472 ment systems, the data from which were combined to  
473 form a complete hourly time series record for each  
474 experimental period. No  $\text{CO}_2$  fluxes were measured  
475 during ABRACOS. Therefore, this data set is used to

476 evaluate the model simulations of the water and en-  
477 ergy budgets after introducing a complex photosyn-  
478 thesis process, and to compare the model simulations  
479 with two different stomatal conductance parameteri-  
480 zations.

### 6.2. Manaus Eddy Covariance Study (1996)

481  
482 Another data set used for this paper was obtained  
483 from an Eddy Covariance Study which was conducted  
484 from 6 July 1995 to 24 August 1996 in the Reserva  
485 Biologica do Cuieiras ( $2^{\circ}35'22''S$ ,  $60^{\circ}6'55''W$ ), some  
486 60 km north of Manaus (Malhi et al., 1998). This is  
487 part of a very extensive, continuous area of dense low-  
488 land terra firm tropical rain forest. Vegetation of the  
489 site is very similar to the site studied by Fan et al.  
490 (1995). One of the primary focuses in the measure-  
491 ment is to examine and describe the nature and mag-  
492 nitude of the diurnal  $\text{CO}_2$  flux and its relationship to  
493 meteorological conditions (Williams et al., 1998). The  
494 fluxes were measured in an Edisol Eddy covariance  
495 system (Malhi et al., 1998). Meteorological data were  
496 collected with an automatic weather station. The gas  
497 analyzers were calibrated at least weekly using zero  
498 and fixed concentration  $\text{CO}_2$  and water vapor sam-  
499 ples. Very little drift in analyzer concentration was  
500 noted over a diurnal cycle or on a week-to-week ba-  
501 sis. Real time data were collected as 10 min average.  
502 Corrections were applied for the dampening of fluc-  
503 tuations at high frequencies using the approach out-  
504 lined by Moore (1986) and Moncrieff et al. (1997).  
505 For the study in this paper, the data collected only  
506 from late December 1995 to mid-January, 1996 were  
507 used because of the better continuity and certainty of  
508 biophysical parameters. For convenience, this data set  
509 is called “Manaus data”.

## 510 7. Results and discussion

511 The SSiB model will be used to study the impact  
512 of land cover change in Amazonia region on the re-  
513 gional climate and carbon balance using the Collatz  
514 et al. photosynthesis and stomatal conductance model.  
515 Thus, proper simulations in both carbon flux and heat  
516 fluxes are necessary. The original SSiB model using  
517 the empirical Jarvis stomatal model (SSiB.0) has pro-  
518 duced reasonable simulations of heat fluxes in the

519 off-line tests for Amazon sites (e.g. Xue et al., 1991,  
520 1996a). As the first step, we must check whether the  
521 more realistic but more complex approach for simula-  
522 tion of stomatal control is still able to yield reasonable  
523 simulations in heat fluxes. Then we will evaluate how  
524 the two modified SSiB versions (SSiB\_1 and SSiB\_2)  
525 perform for the CO<sub>2</sub> flux simulations.

### 526 7.1. Simulation of heat fluxes (SSiB\_0, SSiB\_1 and 527 SSiB\_2 versus observations)

528 In the off-line numerical experiments, we used ob-  
529 served temperature, humidity, and wind speed at the  
530 reference height, precipitation and net radiation at the  
531 surface as forcing to test SSiB. SSiB calculates en-  
532 ergy components, including the latent heat, sensible  
533 heat, and ground heat fluxes, momentum flux, canopy  
534 photosynthesis, and upward short wave and long wave  
535 radiation. All of these components, except long wave  
536 radiation, were measured during ABRACOS field ex-  
537 periments. The values of vegetation parameters used  
538 for this off-line validation were from measurements  
539 in the ABRACOS field campaign and are listed in  
540 Table 3.

541 ABRACOS intensive flux observations were made  
542 for a continuous 30-day period during Mission 1 (M1)  
543 and for 74 days during Mission 2 (M2). Figs. 4 and 5

Table 3  
Vegetation parameters of the ABRACOS data set

Vegetation parameters	Values
Surface albedo	0.18
Leaf area index (LAI)	1 (M1), 2 (M2)
Greenness	0.7 (M1), 0.9 (M2)
Vegetation cover fraction	0.85
Soil layer thicknesses (m)	0.02, 0.98, 1
Soil hydraulic conductivity at saturation (ms <sup>-1</sup> )	2.2e <sup>-5</sup>
Sorption parameter, <i>B</i>	6.9
Soil water potential at saturation (m)	-0.035
Porosity	0.59
Minimum stomatal resistance (sm <sup>-1</sup> )	140
Adjustment factor for water vapor deficit	0.020
Adjustment factor for temperature	295, 276, 323
Adjustment factor for soil moisture	1.73, 5.8
Rooting depth (m)	1.0
Surface roughness length (m)	0.026
Displacement height (m)	0.18
Vegetation height (m)	0.28

Table 4  
Correlation coefficients between the hourly output of heat fluxes from the three model versions and the field observations

Flux	Model	ABRACOS Mission 1 (M1)	ABRACOS Mission 2 (M2)	Manaus
<i>H</i>	SSiB_0	0.87	0.91	0.86
	SSiB_1	0.88	0.90	0.91
	SSiB_2	0.88	0.89	0.91
<i>LE</i>	SSiB_0	0.94	0.96	0.96
	SSiB_1	0.94	0.97	0.97
	SSiB_2	0.94	0.95	0.98
<i>G</i>	SSiB_0	0.83	0.91	0.91
	SSiB_1	0.82	0.90	0.73
	SSiB_2	0.82	0.83	0.84

544 are the comparisons between the observed and sim-  
545 ulated daily means of latent heat, sensible heat and  
546 soil heat fluxes for three versions of the SSiB model  
547 (SSiB\_0, SSiB\_1 and SSiB\_2). The correlation coeffi-  
548 cients of the daily mean fluxes for the entire periods of  
549 both M1 and M2 are listed in Table 4. The three ver-  
550 sions of SSiB produce very similar simulations for the  
551 three fluxes. Fig. 5a shows that in M2 the simulated  
552 latent heat flux closely follows observations. The ob-  
553 served latent heat fluxes dropped sharply several times  
554 during M2 (3, 4, and 25 August and 2 September).  
555 The model simulated these dramatic changes and re-  
556 covered very well. In M1, although the three versions  
557 of the model generally followed the trend, the sim-  
558 ulations of the three heat fluxes fluctuated about the  
559 observations (Fig. 4). In the early October, the mod-  
560 els underestimated latent heat flux and overestimated  
561 sensible heat flux by about 30%. But in the middle  
562 October, the model overestimated latent heat flux  
563 and underestimated sensible heat flux by about 20%.  
564 These fluctuations might result from the biases of soil  
565 heat flux simulations from their observations (Fig. 4c).  
566 In general, the simulations of the heat fluxes from  
567 the two modified SSiB versions (SSiB\_1 and SSiB\_2)  
568 are very similar to those from the original SSiB  
569 (SSiB\_0).

570 For the Manus data set, detailed soil and vegetation  
571 information was not available except that the vegeta-  
572 tion cover of the study site is a continuous area of  
573 dense lowland terra firm tropical rainforest and that  
574 the leaf area index was 5–6 and canopy height 30 m  
575 according to Malhi et al. (1998). In an off-line test,  
576 it is important to have a proper set of vegetation and  
577

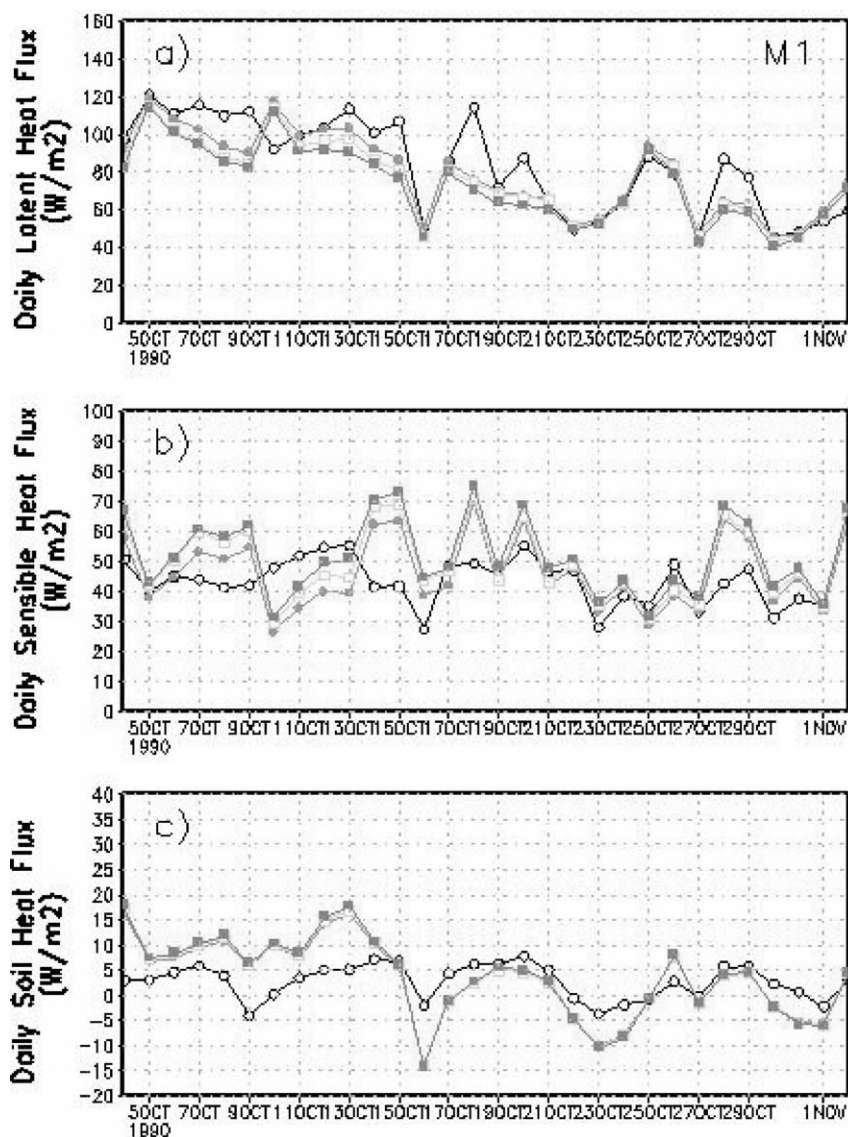


Fig. 4. The daily mean values of (a) latent heat flux, (b) sensible heat flux, and (c) soil heat flux obtained from the observations during the Mission 1 of the ABRACOS field experiment (line marked with open circles), the simulations of SSiB.0 (solid squares), the simulations of SSiB.1 (solid circles) and the simulations of SSiB.2 (open squares). If solid circles or open squares are not seen, they are overlaid by solid squares.

577 soil parameters and it may cause systematic errors if  
 578 these parameters are not setup correctly (Xue et al.,  
 579 1996b; Xue et al., 1997). Because we have no mea-  
 580 sured surface vegetation and soil information, we use  
 581 the vegetation and soil parameters from a vegetation  
 582 and soil parameter table, which is used in the cou-

583 pled atmospheric/SSiB model (e.g. Xue et al., 2001).  
 584 In this study, we base on the above-mentioned veg-  
 585 etation type information to specify the land parame-  
 586 ter values. Fig. 6 shows the result from three versions  
 587 of SSiB. It is evident that all three versions are able  
 588 to simulate the variability in latent heat, sensible heat

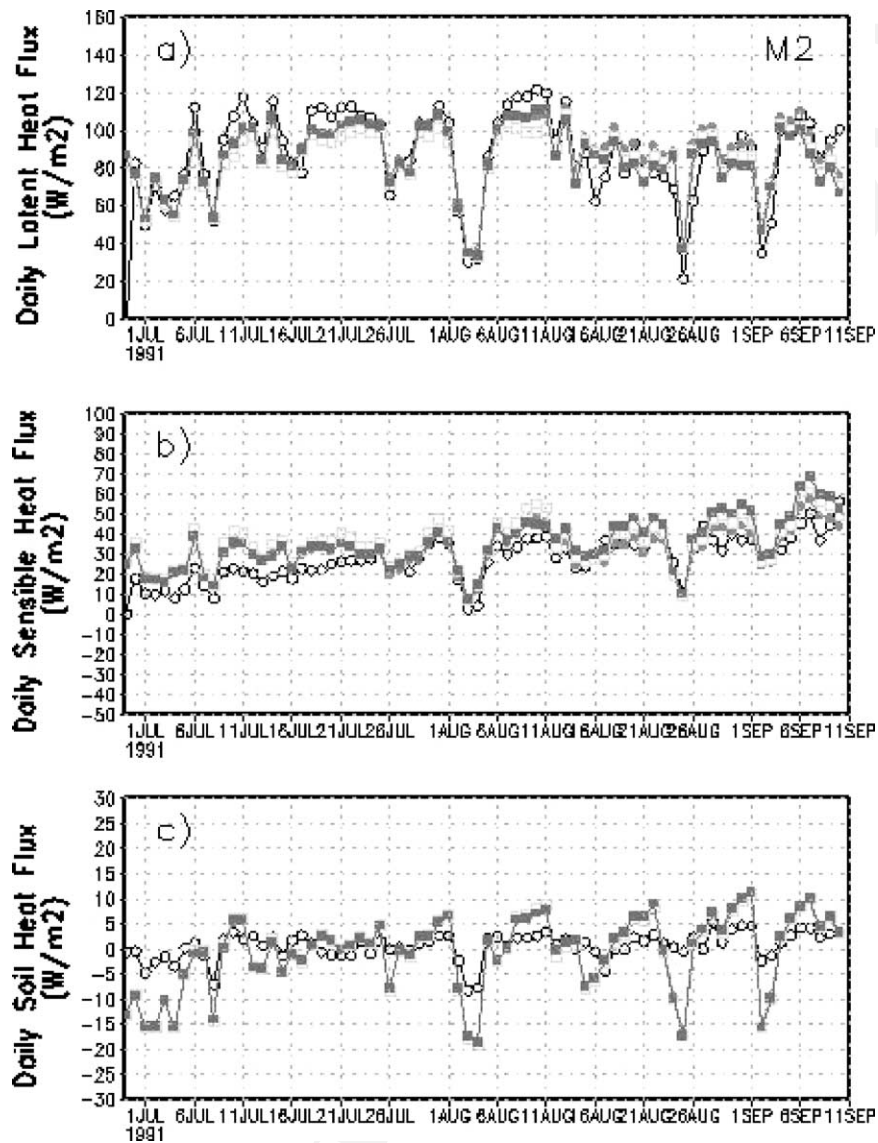


Fig. 5. The daily mean values of (a) latent heat flux, (b) sensible heat flux, and (c) soil heat flux obtained from the observations during the Mission 2 of the ABRACOS field experiment (line marked with open circles), the simulations of SSiB\_0 (solid squares), the simulations of SSiB\_1 (solid circles) and the simulations of SSiB\_2 (open squares). If solid circles or open squares are not seen, they are overlaid by solid squares.

589 and soil heat fluxes well. The correlations between the  
 590 model outputs and the field observations are similar to  
 591 the results for the ABRACOS data sets (Table 4). This  
 592 result further indicates that the two modified versions  
 593 of SSiB do not compromise the capability of the orig-  
 594 inal SSiB in simulating the latent heat, sensible heat  
 595 and soil heat fluxes.

## 7.2. Simulations of $CO_2$ flux (SSiB\_1 and SSiB\_2 versus observations) 596 597

The primary goal of this work is to enhance the  
 598 SSiB model with  $CO_2$  flux simulation capability. How  
 599 the two modified versions of the SSiB model per-  
 600 form in  $CO_2$  flux simulation is of the most concern. 601

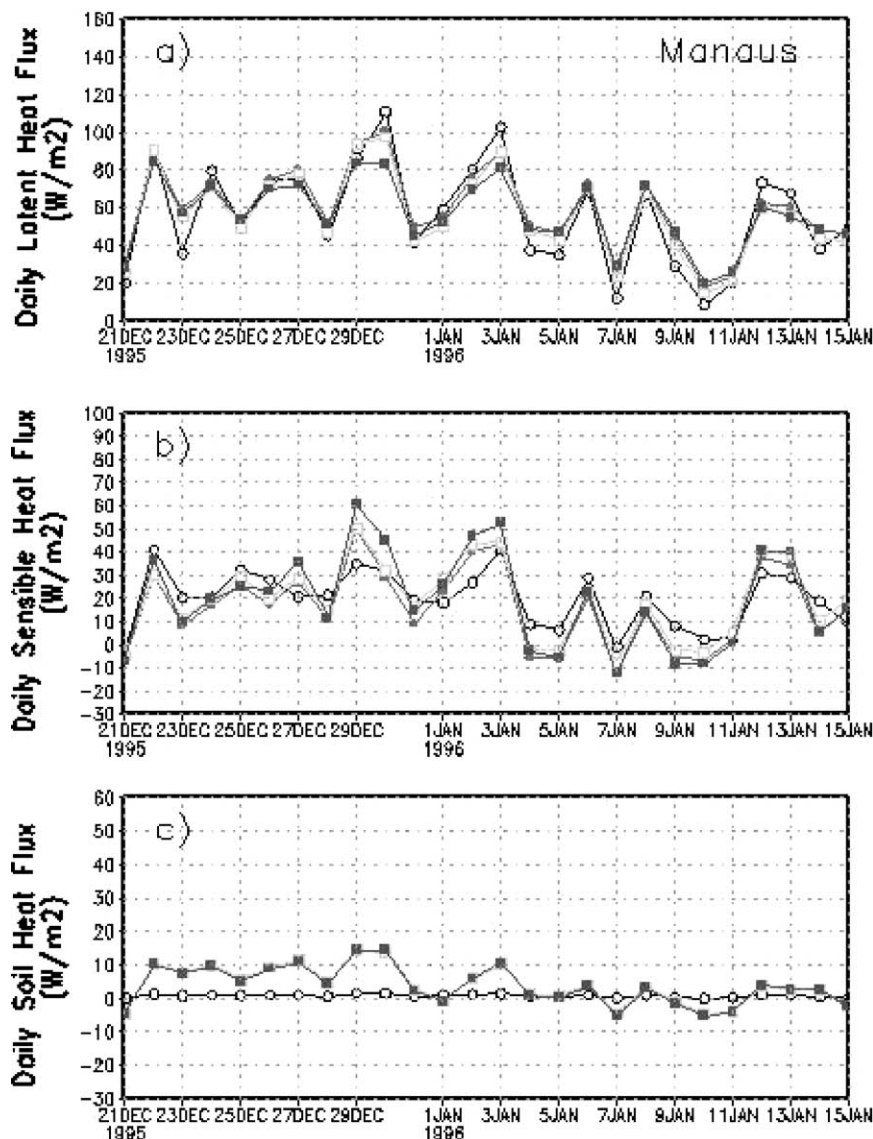


Fig. 6. The daily mean values of (a) latent heat flux, (b) sensible heat flux, and (c) soil heat flux obtained from the observations during the Eddy Covariance Study (line marked with open circles), the simulations of SSiB.0 (solid squares), the simulations of SSiB.1 (solid circles) and the simulations of SSiB.2 (open squares). If solid circles or open squares are not seen, they are overlaid by solid squares.

602 Using the only  $CO_2$  flux measurements in the Man-  
 603 aus data set, we can find the answer to this ques-  
 604 tion from the results demonstrated in the following  
 605 figures.

606 Fig. 7 is a comparison between the simulations  
 607 (marked with solid) circles) by (a) SSiB.1 or (b)  
 608 SSiB.2 and their corresponding observations (open

609 circles) of the above canopy hourly  $CO_2$  flux for  
 610 the 26 days in the Manaus data set. The correlation  
 611 coefficient between the hourly simulation and field  
 612 observation is 0.73 for SSiB.1 and 0.84 for SSiB.2.  
 613 Although both SSiB.1 and SSiB.2 simulated the  
 614 diurnal cycles of the  $CO_2$  flux, the simulations by  
 615 SSiB.1, which uses the same leaf to canopy scaling

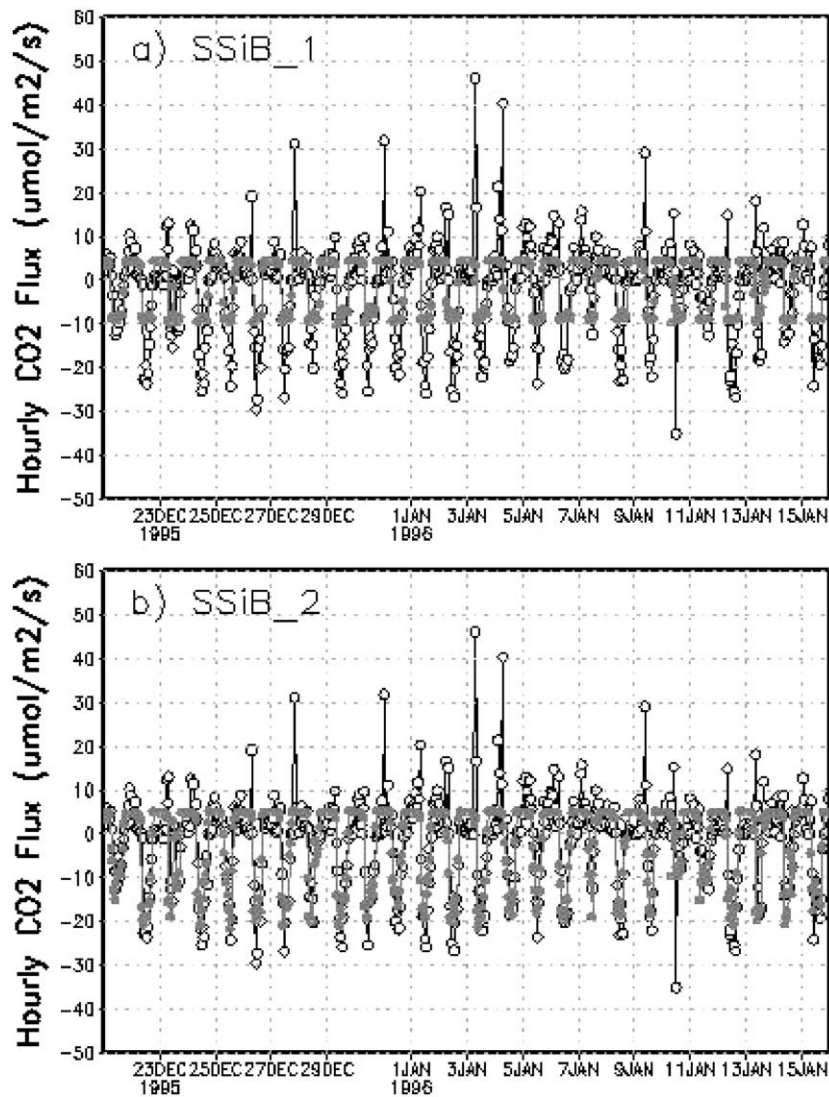


Fig. 7. The hourly above canopy CO<sub>2</sub> flux simulations (solid circles) and their field observations (open circles) for the 26-day data set from the Manaus Eddy Covariance Study: (a) for SSiB.1; (b) for SSiB.2. Negative value means that CO<sub>2</sub> is transported from the above canopy atmosphere downward to the canopy.

616 strategy as in SSiB.2 (Sellers et al., 1996a), have very  
 617 similar maximums during midday for all 26 days.  
 618 The simulations by SSiB.2, which computes net pho-  
 619 tosynthetic rate and stomatal conductance for sunlit  
 620 and shaded leaves, respectively, have diurnal cycles  
 621 varying mainly with incoming photosynthetically ac-  
 622 tive radiation. The observed diurnal cycles of CO<sub>2</sub>  
 623 flux follow the PAR diurnal pattern. Thus, the SSiB.2

624 simulations have a higher correlation coefficient  
 625 (0.84).

626 Fig. 8 is the diurnal cycles of the model simulations  
 627 plotted against the field observations averaged over  
 628 the 26 days. Despite general consistency of the simu-  
 629 lations of both SSiB.1 and SSiB.2 with observations,  
 630 a noontime square wave in the simulations of SSiB.1  
 631 is evident. To more clearly examine the difference in

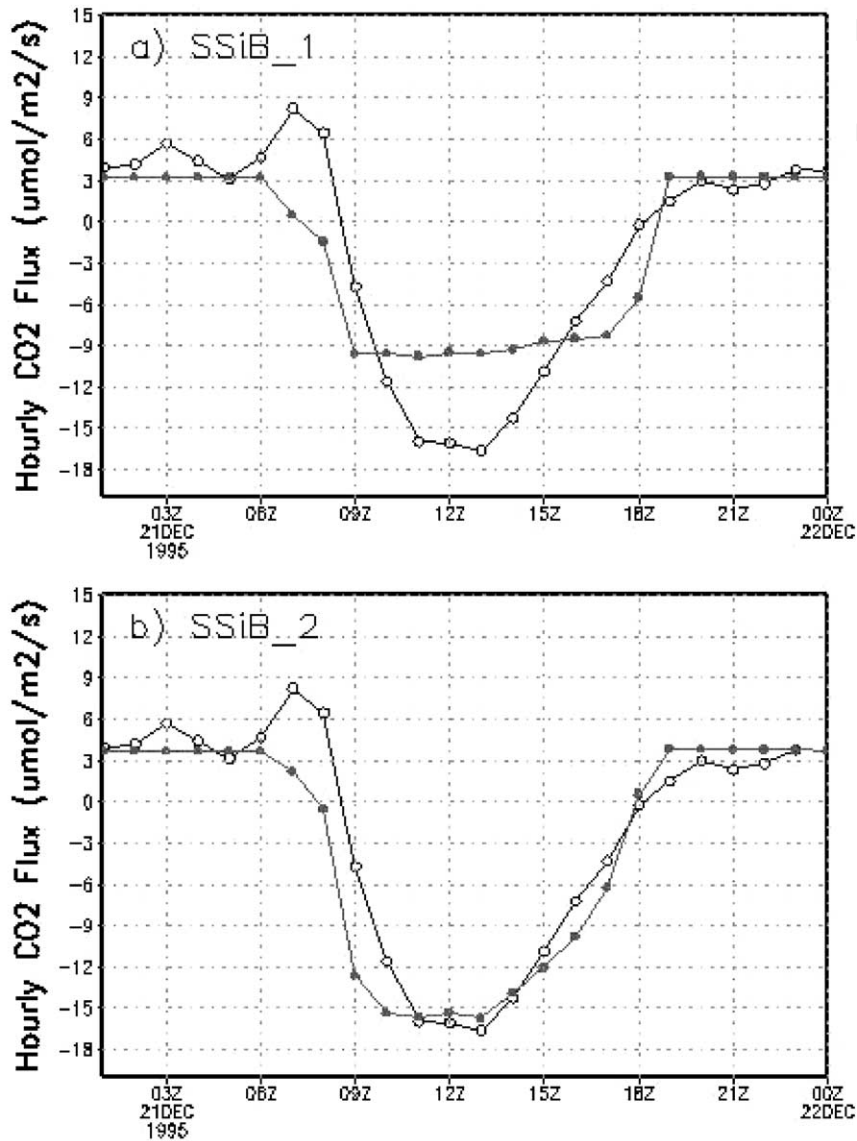


Fig. 8. The averaged diurnal curve of the above canopy CO<sub>2</sub> flux simulations (solid circles) and their field observations (open circles) for the 26-day data set from the Manaus Eddy Covariance Study: (a) for SSiB-1; (b) SSiB-2. Negative value means that CO<sub>2</sub> is transported from the above canopy atmosphere downward to the canopy.

632 the CO<sub>2</sub> flux diurnal cycle simulations by SSiB-1 and  
 633 SSiB-2, the simulated plant photosynthetic rate  $A_n$   
 634 and their three limitations (namely, the RuBP saturation  
 635 limited rate  $W_c$ , the electron transportation limited  
 636 rate  $W_e$ , and the sink limited rate  $W_s$ ) averaged  
 637 over the 26 days are plotted in Fig. 9 for SSiB-1 and  
 638 Fig. 10 for SSiB-2. As in Eq. (4), the photosynthetic

rate  $A_n$  is the minimum of these three limitations ad- 639  
 justed with a quadratic equation (Collatz et al., 1991). 640  
 Thus, the curve of net photosynthetic rate  $A_n$  in Fig. 9 641  
 goes beneath the lowest of  $W_c$ ,  $W_e$  and  $W_s$ . For most 642  
 of the day-time,  $W_c$  simulated by SSiB-1 is the lowest 643  
 and does not change much for more than 6 h around 644  
 noontime. Thus, the net photosynthetic rate  $A_n$  follows 645

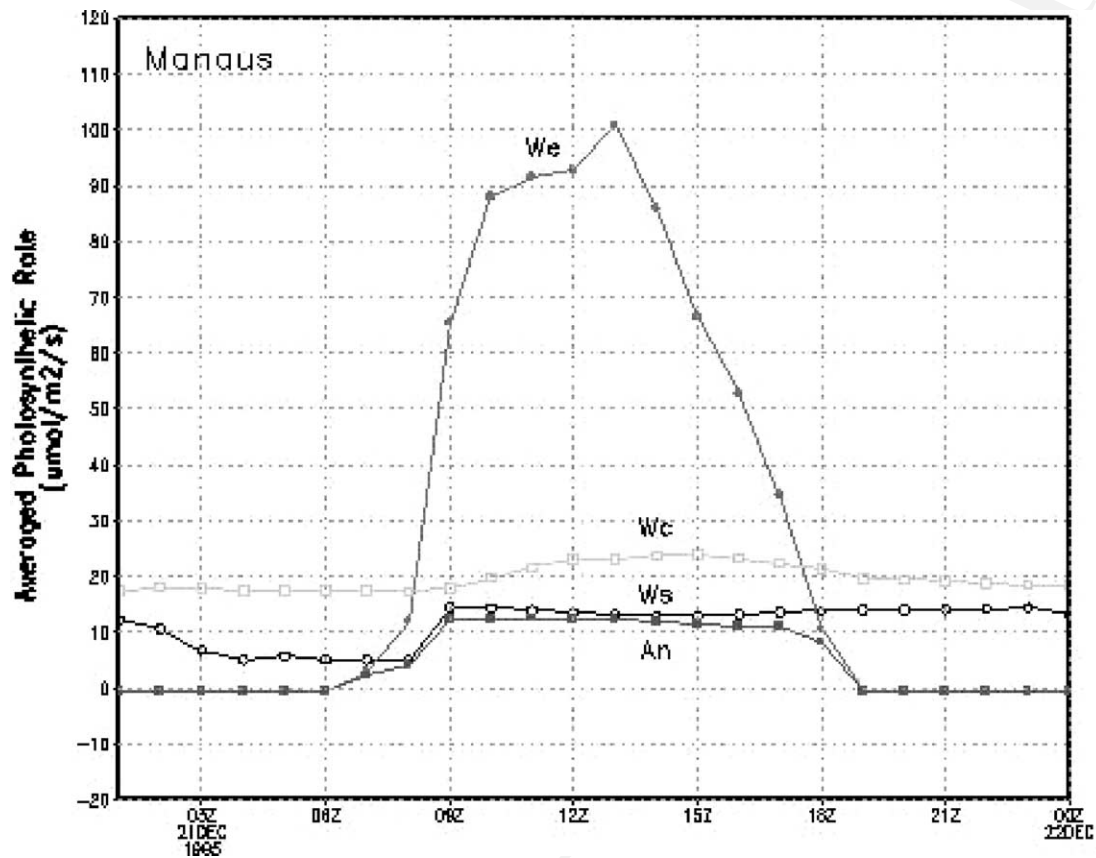


Fig. 9. The averaged diurnal curve of the canopy  $\text{CO}_2$  photosynthetic rate and its three components simulated by Phost.1. Canopy net photosynthesis rate  $A_n$  is marked with solid squares. The Rubisco limitation  $W_c$  is open circles. The PAR limitation  $W_e$  is solid circles. The sink limitation  $W_s$  is open squares.

646  $W_c$  and shows a day-time square wave. This day-time  
 647 square wave is not consistent with observations well  
 648 documented in the literature (Thornley and Johnson,  
 649 1990). One of the reasons for this incorrect simulation  
 650 by SSiB.1 in Fig. 9 may be that the parameters  
 651 of the Collatz et al. model were setup incorrectly so  
 652 that the simulations of  $W_e$  are too large or the com-  
 653 puted values of  $W_c$  or  $W_s$  are too small. However,  
 654 as stated in Section 5, an apparent reason for the in-  
 655 correct simulation of SSiB.1 is the strategy of scal-  
 656 ing the Collatz et al. model from leaf to canopy in  
 657 Sellers et al. (1996a). The scaling-up method treats all  
 658 leaves within the plant canopy the same way. This may  
 659 have underestimated the light saturation phenomenon  
 660 of plant leaves (Chen et al., 1999). This underestima-  
 661 tion of light situation may have caused the simulation

of  $W_e$  being too high. SSiB.2 attempts to avoid this  
 problem by implementing the Collatz et al. model to  
 sunlit leaves and shaded leaves separately. The results  
 shown in Figs. 7b and 8b from SSiB.2 demonstrated  
 significant improvement.

Fig. 10 plots the daily above canopy  $\text{CO}_2$  flux aver-  
 ages of the model simulations and their field obser-  
 vations. For SSiB.1, because of the unrealistic square  
 wave in the diurnal variation of plant photosynthetic  
 rate, the simulated daily above canopy  $\text{CO}_2$  flux aver-  
 ages (solid circles) do not match the observations  
 well (open circles). For SSiB.2, its simulations (open  
 squares) improve obviously over the simulation by  
 SSiB.1. The correlation coefficient between the aver-  
 ages of the simulated daily above canopy  $\text{CO}_2$  flux  
 and their corresponding observations is only 0.42 for

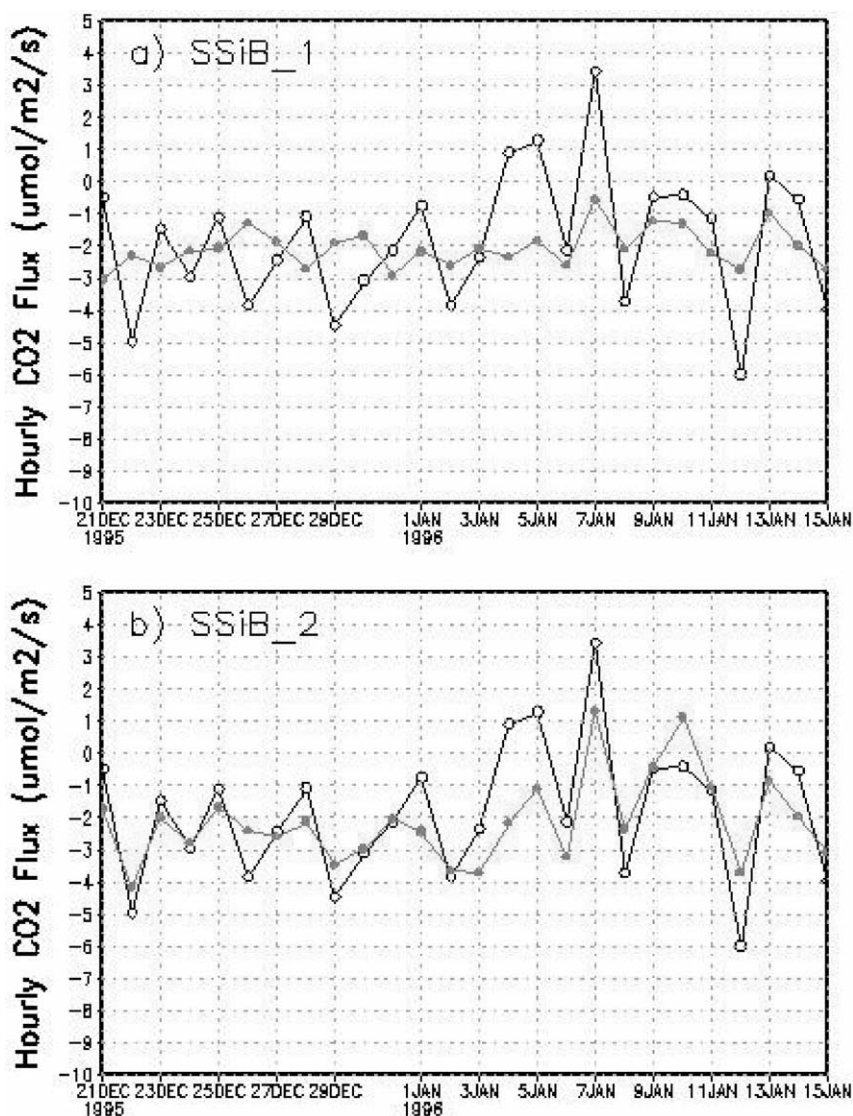


Fig. 10. The daily means of the above canopy CO<sub>2</sub> flux simulations (solid circles) and their field observations (open circles) for the 26-day data set from the Manaus Eddy Covariance Study: (a) for SSiB\_1; (b) for SSiB\_2. Negative value means that CO<sub>2</sub> is transported from the above canopy atmosphere downward to the canopy.

678 SSiB\_1 and 0.80 for SSiB\_2. In this paper, we set the  
 679 soil respiration rate as a constant. It will be the fo-  
 680 cus of further studies to improve the capability of the  
 681 SSiB model in CO<sub>2</sub> flux simulations. With a more  
 682 realistic simulation of  $F_{cs}$  in Eq. (18), the simula-  
 683 tion result of  $F_{ca}$  by SSiB\_2 is expected to be even  
 684 better.

## 8. Conclusions

Using three data sets collected from two large-scale  
 field experiments, this study aims to improve the so-  
 lution experiments, this study aims to improve the so-  
 lution method and scaling-up approach of the Collatz  
 et al. model of plant photosynthesis and stomatal con-  
 ductance in order to implement the model in the SSiB

685

686

687

688

689

690

691 for CO<sub>2</sub> flux simulations. From the results obtained  
692 we can make the following conclusions:

- 693 (1) The Collatz et al. model of plant photosynthe-  
694 sis and stomatal conductance can solved with  
695 a semi-analytic method, which brings with bet-  
696 ter computational efficiency and stability for  
697 the coupled land surface–atmosphere interaction  
698 models.  
699 (2) Implementation of the analytic solution approach  
700 for CO<sub>2</sub> flux solution in the SSiB model produces  
701 reasonable simulations of latent heat, sensible heat  
702 and soil heat fluxes and enhances the SSiB into a  
703 new generation model.  
704 (3) The leaf to canopy scaling-up strategy used in  
705 [Sellers et al. \(1996a\)](#) for the implementation of the  
706 Collatz et al. model results in a day-time square  
707 wave in the net photosynthetic rate simulations.  
708 Considering the sunlit leaves and shaded leaves  
separately in the Collatz et al. model implemen-

tation in the SSiB model improves the photosyn- 709  
thesis and CO<sub>2</sub> flux simulations significantly. 710

**Acknowledgements**

711  
712 The authors would like to thank Dr. John Grace, Dr.  
713 Yadvinder Malhi of University of Edinburgh in United  
714 Kingdom and Dr. Antonio D. Nobre of Centro de Pre-  
715 visao de Tempo e Estudos Climaticos, Brazil, for pro-  
716 viding field observation data of the Manaus Eddy Co-  
717 variance study. Drs. J. Gash and H. G. Basetable of  
718 the Institute of Hydrology (UK) and their Brazilian  
719 collaborators are thanked for compiling and provid-  
720 ing the ABRACOS data. This study was supported  
721 by NASA’s grant of the LBA-Hydrometeorology pro-  
722 gram (NASA Grant NAG59386). The authors would  
723 also like to thank the anonymous reviewers and the  
724 editor for their constructive comments and recommen-  
725 dations.

**Appendix A. List of symbols with units and definition**

Symbol	Units	Definition
$A_n$	$\mu\text{mol m}^{-2} \text{s}^{-1}$	Net CO <sub>2</sub> assimilation of the canopy
$A, A_i (i = 1, \dots, 7), a_c$		Interim variables for the analytic solutions
$B, B_1, B_2, b_c$		Interim variables for the analytic solutions
$b$	$\mu\text{mol m}^{-2} \text{s}^{-1}$	Coefficient in Eq. (3) (0.01 for C <sub>3</sub> , 0.04 for C <sub>4</sub> vegetation)
$C, c_c$		Interim variables for the analytic solutions
$C_a$	Pa	CO <sub>2</sub> concentration of the atmosphere
$C_i$	Pa	CO <sub>2</sub> concentration inside plant leaves
$C_s$	Pa	CO <sub>2</sub> concentration at leaf surface
$C_1, C_2$		Empirical coefficients of soil moisture adjustment factor, Eq. (19)
$e_a$	Pa	Water vapor pressure at the reference height
$e^*(T)$	Pa	Saturation vapor pressure at temperature $T$
$e_s$	Pa	Water vapor pressure at leaf surface
$\varepsilon_3/\varepsilon_4$	$\text{mol mol}^{-1}$	Intrinsic quantum efficiency of leaf photosynthesis for C <sub>3</sub> /C <sub>4</sub> plant*
$F_{ca}$	$\mu\text{mol m}^{-2} \text{s}^{-1}$	CO <sub>2</sub> flux above land surface
$F_{cs}$	$\mu\text{mol m}^{-2} \text{s}^{-1}$	CO <sub>2</sub> flux from the soil surface
$F$	$\text{m}^2 \text{m}^{-2}$	Canopy leaf area index
$F_{shd}$	$\text{m}^2 \text{m}^{-2}$	Shaded leaf area index
$F_{slt}$	$\text{m}^2 \text{m}^{-2}$	Sunlit leaf area index
$f_d$		Fraction of diffusive radiation in total radiation
$f(\psi)$		Adjustment factor to count for soil moisture effect

## Appendix A. (Continued)

Symbol	Units	Definition
$G(\mu)$		Projection of leaves in direction of incoming radiation flux*
$g_b$	$\mu\text{mol m}^{-2} \text{s}^{-1}$	Leaf boundary layer aerodynamic conductance
$g_s$	$\mu\text{mol m}^{-2} \text{s}^{-1}$	Stomatal conductance to latent and sensible heat transfer
$\Gamma^*$	$\mu\text{mol mol}^{-1}$	The $\text{CO}_2$ compensation point of the leaves*
$\gamma$	$\text{Pa K}^{-1}$	Psychrometric constant
$h_s$		Relative humidity within the leaf surface boundary layer
$K_c$	$\mu\text{mol mol}^{-1}$	Michaelis-Menten competitive inhibition constant for $\text{CO}_2^*$
$K_o$	$\mu\text{mol mol}^{-1}$	Michaelis-Menten competitive inhibition constant for $\text{O}_2^*$
$\bar{k}$		Time-mean value of radiation extinction coefficient*
$m$		Coefficient in Eq. (3) (9 for $\text{C}_3$ , 4 for $\text{C}_4$ vegetation)
$N$		Canopy green leaf fraction
$O_i$	$\mu\text{mol mol}^{-1}$	Internal $\text{O}_2$ concentration of the leaves
$P$		Interim variables for the analytic solutions
PAR, $\text{PAR}_0$	$\mu\text{mol m}^{-2} \text{s}^{-1}$	Photosynthetically active radiation above the canopy
$\text{PAR}_{\text{dr}}$	$\mu\text{mol m}^{-2} \text{s}^{-1}$	Direct photosynthetically active radiation above the canopy
$\text{PAR}_{\text{df}}$	$\mu\text{mol m}^{-2} \text{s}^{-1}$	Diffusive photosynthetically active radiation above the canopy
$\text{PAR}_{\text{sIt}}$	$\mu\text{mol m}^{-2} \text{s}^{-1}$	PAR received by sunlit leaves
$\text{PAR}_{\text{shd}}$	$\mu\text{mol m}^{-2} \text{s}^{-1}$	PAR received by shaded leaves
$p$	Pa	Air pressure
$\psi$	Pa	Soil water potential
$\Pi$		Leaf to canopy scaling factor (see Eq. (12))
$Q$		Interim variables for the analytic solutions
$R_d$	$\mu\text{mol m}^{-2} \text{s}^{-1}$	The dark respiration rate of the canopy
$r_a$		Aerodynamic resistance of the air above the canopy to the measurement height
$\rho c_p$	$\text{J m}^{-3} \text{K}^{-1}$	Volumetric heat capacity of air
$T_a$	$^{\circ}\text{C}$	Air temperature at the reference height
$T_c$	$^{\circ}\text{C}$	Integrated leaf temperature of the canopy
$\theta_s$	$^{\circ}$	Sun elevation angle
$\theta_{\text{ls}}$	$^{\circ}$	Mean angle between leaf normal and sunlight
$\mu$		Direction of incoming radiation flux
$V_{\text{max}}$	$\mu\text{mol m}^{-2} \text{s}^{-1}$	Maximum RuBP carboxylation rate
$V$		Canopy cover fraction
$W_c$	$\mu\text{mol m}^{-2} \text{s}^{-1}$	Rubisco-limited rate of $\text{CO}_2$ assimilation
$W_e$	$\mu\text{mol m}^{-2} \text{s}^{-1}$	Electron transportation limited $\text{CO}_2$ assimilation rate
$W_s$	$\mu\text{mol m}^{-2} \text{s}^{-1}$	Product sink limited rate of $\text{CO}_2$ assimilation
$\omega\Pi$		Leaf-scattering coefficient for PAR (Sellers et al., 1996a)

726 **Appendix B. Analytical solutions of Eq. (14)**

727 In Eq. (14)

728  $A = A_3 A_6 m h_s g_b^2 p + A_3 B_1 b g_b F$  (A.1)  
729

730  $B = g_b p (A_6 ((1.6 - m h_s) B_1 + A_4 m h_s g_b)$   
731  $+ A_3 A_7 m h_s g_b) + b F (A_4 B_1 g_b$   
732  $+ A_3 B_2 g_b - B_1^2)$  (A.2)  
733

734  $C = g_b p (A_6 (1.6 - m h_s) B_2 + A_7 (1.6 - m h_s) B_1$   
735  $+ A_4 m h_s g_b) + b F (A_4 B_2 g_b - 2 B_1 B_2)$  (A.3)

736  $D = A_7 B_2 (1.6 - m h_s) g_b p - B_2^2 b F$  (A.4)

737 and

738  $A_6 = A_1 + A_3 A_5$  (A.5)

739  $A_7 = A_4 A_5 - A_1 A_2$  (A.6)

740  $B_1 = C_a g_b A_3 - 1.4 p A_6$  (A.7)

741  $B_2 = C_a g_b A_4 - 1.4 p A_7$  (A.8)

742  $h_s = e_s / e_s^* (T_c)$  (A.9)

743 If we define  $P = (C/A) - (B^2/3A^2)$  and  $Q =$   
744  $(D/A) + (2B^3/27A^3) - (BC/3A^2)$ , then the discrim-  
745 inator of Eq. (14) is

746  $\Delta = \left(\frac{Q}{2}\right)^2 + \left(\frac{P}{3}\right)^3$  (A.10)

747 If ( $\Delta \geq 0$ ), the cubic Eq. (14) has only one valid solu-  
748 tion. If ( $\Delta < 0$ ), Eq. (14) yields three roots. These  
749 roots can be computed with equations listed in most  
750 mathematical handbooks. The valid solution is the posi-  
751 tive minimum of the three, that is

752  $C_i = \min(x_1, x_2, x_3)$  (A.11)

753 If  $A_1 \neq 0$  and  $A_3 = 0$  in Eq. (13), Eq. (14) becomes  
754 the following quadratic equation:

755  $a_c C_i^2 + b_c C_i + c_c = 0$  (A.12)

756 where

758  $a_c = g_b p A_1 (1.4 p A_1 (1.6 - m h_s) - m h_s g_b)$   
759  $+ b F (1.4 p A_1 (1.4 p A_1 + g_b))$  (A.13)

$b_c = -g_b p A_1 1.4 p A_1 (C_a g_b - 1.4 p A_5)$  761  
 $+ A_5 g_b p (1.4 p A_1 (1.6 - m h_s) - m h_s g_b)$  762  
 $+ b F (2.8 p A_1 + g_b) (C_a g_b - 1.4 p A_5)$  (A.14) 763  
764

$c_c = -g_b p A_5 (1.6 - m h_s) (C_a g_b - 1.4 p A_5)$  765  
 $+ b F (C_a g_b - 1.4 p A_5)^2$  (A.15) 766

The discriminator of Eq. (A.12) is

$\Delta_2 = b_c^2 - 4 a_c c_c$  (A.16) 768

When ( $\Delta_2 \geq 0$ ), the quadratic equation has two roots. 769  
These two roots can be computed with equations listed 770  
in most mathematical handbooks. The minimum of 771  
them is the valid value for  $C_i$  if it is greater than zero, 772  
that is 773

$C_i = \min(x_1, x_2)$  (A.17) 774

If  $\Delta_2 < 0$ , then the equation has no valid solutions. 775

**References** 776

Baldocchi, D., 1994. An analytical solution for coupled leaf 777  
photosynthesis and stomatal conductance models. *Tree Physiol.* 778  
14, 1069–1079. 779  
Ball, J.T., 1988. An Analysis of Stomatal Conductance. Ph.D. 780  
Dissertation, Stanford University, Stanford, CA, 89 p. 781  
Bastable, H.G., Shuttleworth, W.J., Dallarosa, R.L.G., Fisch, G., 782  
Nobre, C.A., 1993. Observations of climate, albedo, and surface 783  
radiation over cleared and undisturbed Amazonian forest. *Int.* 784  
*J. Climatol.* 13, 783–798. 785  
Bonan, G.B., 1995. Land-atmosphere CO<sub>2</sub> exchange simulated by 786  
a land surface process model coupled to an atmospheric general 787  
circulation model. *J. Geophys. Res.* 100, 2817–2831. 788  
Boonen, C., Samson, R., Janssens, K., Pien, H., Lemeur, R., 789  
Berckmans, D., 2002. Scaling the spatial distribution of 790  
photosynthesis from leaf to canopy in a plant growth chamber. 791  
*Ecol. Model.* 156 (2/3), 201–212. 792  
Chen, J.M., Liu, J., Cihlar, J., Goulden, M.L., 1999. Daily canopy 793  
photosynthesis model through temporal and spatial scaling for 794  
remote sensing applications. *Ecol. Model.* 124, 99–119. 795  
Chou, S.C., Tanajura, C.A.S., Xue, Y., Nobre, C.A., 2002. 796  
Simulations with the coupled Eta/SSiB model over South 797  
America. *J. Geophys. Res.*, submitted for publication. 798  
Collatz, G.J., Grivet, C., Ball, J.T., Berry, J.A., 1991. Physiological 799  
and environmental regulation of stomatal conductance, 800  
photosynthesis and transpiration: a model that includes a 801  
laminar boundary layer. *Agric. For. Meteorol.* 54, 107–136. 802  
Collatz, G.J., Ribas-Carbo, M., Berry, J.A., 1992. Coupled 803  
photosynthesis-stomatal conductance model for leaves of C<sub>4</sub> 804  
plants. *Aust. J. Plant Physiol.* 19, 519–538. 805

- 806 Cox, P.M., Betts, R.A., Jones, C.D., Spall, S.A., Totterdell, I.J.,  
807 2000. Acceleration of global warming due to carbon cycle  
808 feedbacks in a coupled climate model. *Nature* 408, 184–187.
- 809 Denning, A.S., Collatz, G.J., Zhang, C., Randall, D.A., Berry, J.A.,  
810 Sellers, P.J., Colello, G.D., Dazlich, D.A., 1996a. Simulations  
811 of terrestrial carbon metabolism and atmospheric CO<sub>2</sub> in a  
812 general circulation model. Part I. Surface carbon fluxes. *Tellus*  
813 48B, 521–542.
- 814 Denning, A.S., Randall, D.A., Collatz, G.J., Sellers, P.J., 1996b.  
815 Simulations of terrestrial carbon metabolism and atmospheric  
816 CO<sub>2</sub> in a general circulation model. Part 2. Simulated CO<sub>2</sub>  
817 concentration. *Tellus* 48(B), 543–567.
- 818 Fan, S.-M., Wofsy, S., Bakwin, P., Jacob, D., 1995.  
819 Atmospheric-biosphere exchange of CO<sub>2</sub> and O<sub>3</sub> in the central  
820 Amazon forest. *J. Geophys. Res.* 95, 16851–16864.
- 821 Farquhar, G.D., von Caemmerer, S., Berry, J.A., 1980. A  
822 biochemical model of photosynthetic CO<sub>2</sub> assimilation in leaves  
823 of C<sub>3</sub> species. *Planta* 149, 78–90.
- 824 Gash, J.H.C., Nobre, C.A., Roberts, J.M., Victoria, R.L., 1996.  
825 Amazonian Deforestation and Climate. Wiley, Chichester,  
826 611 p.
- 827 Henderson-Seller, A., Yang, Z.-L., Dickinson, R.E., 1993. The  
828 project for intercomparison of land-surface parameterization  
829 schemes. *Bull. Am. Meteor. Soc.* 74, 1335–1349.
- 830 Henderson-Seller, A., Pitman, A.J., Love, P.K., Irannejad, P., Chen,  
831 T.H., 1995. The project for intercomparison of land-surface  
832 parameterization schemes (PILPS): phases 2 and 3. *Bull. Am.*  
833 *Meteor. Soc.* 76, 489–503.
- 834 Houghton, R.A., Skole, D.L., Nobre, C.A., 2000. Annual fluxes  
835 or carbon from deforestation and regrowth in the Brazilian  
836 Amazon. *Nature* 403 (6767), 301–304.
- 837 Jarvis, P.G., 1976. The interpretation of the variations in leaf water  
838 potential and stomatal conductance found in canopies in the  
839 field. *Phil. Trans. R. Soc. Lond. Ser. B Biol. Sci.* 273, 593–610.
- 840 Jorgensen, S.E., 1997. Ecological modelling by “Ecological  
841 Modelling”. *Ecol. Model.* 100 (1/3), 5–10.
- 842 Keller, M., Melillo, J., Zamboni de Mello, W., 1997. Trace gas  
843 emissions from ecosystems of the Amazon basin. *Ciência e*  
844 *Cultura J. Brazilian Assoc. Adv. Sci.* 49, 87–97.
- 845 Keller, M., Palace, M., Hurtt, G., 2001. Biomass estimation in the  
846 tapajos National forest, Brazil: examination of sampling and  
847 allometric uncertainties. *For. Ecol. Manage.* 154 (3), 371–382.
- 848 Malhi, Y., Nobre, A.D., Grace, J., Kruijt, B., Pereira, M.G.P.,  
849 Culf, A., Scott, S., 1998. Carbon dioxide transfer over a central  
850 Amazonian rain forest. *J. Geophys. Res.* 103 (D24), 31593–  
851 31612.
- 852 McWilliams, A.L.C., Roberts, J.M., Cabral, O.M.R., Leitao,  
853 M.V.B.R., de Costa, A.C.L., Maitelli, G.T., Zamponi,  
854 C.A.G.P., 1993. Leaf area index and above ground biomass  
855 of terra firm rain forest and adjacent clearings in Amazonia.  
856 *Funct. Ecol.* 7 (3), 310–317.
- 857 Moncrieff, J.B., Massheder, J.M., de Bruin, H., Elbers, J., Friberg,  
858 T., Huesunkveld, B., Kabat, P., Scott, S., Soegaard, H., Verhoef,  
859 A., 1997. A system to measure surface fluxes of momentum,  
860 sensible heat, water vapor and carbon dioxide. *J. Hydrol.*  
861 188/189, 589–611.
- 862 Moore, C.J., 1986. Frequency response corrections for Eddy  
863 correlation systems. *Boundary Layer Meteor.* 37, 17–35.
- Norman, J.M., 1982. Simulation of Microclimates. *Biometeorology* 864  
in Integrated Pest Management. Academic Press, New York, 865  
pp. 65–69. 866
- Phillips, O.L., Malhi, Y., Higuchi, N., Laurance, W.F., Nunez, 867  
P.V., Vasquez, R.M., Laurance, S.G., Ferreira, L.V., Stern, M., 868  
Brown, S., Grace, J., 1998. Changes in the carbon balance 869  
of tropical forests: evidence from long-term plots. *Science* 870  
282 (5388), 439–442. 871
- Shimel, D.S., House, J.I., Hibbard, K.A., Bousquet, P., Ciais, P., 872  
Peylin, P., Braswell, B.H., Apps, M.J., Baker, D., Bondeau, A., 873  
Canadell, J., Churkina, G., Cramer, W., Denning, A.S., Field, 874  
C.B., Friedlingstein, P., Goodale, C., Heimann, M., Houghton, 875  
R.A., Melillo, J.M., Moore, B., Murdiyarso, D., Noble, I., 876  
Pacala, S.W., Prentice, I.C., Raupach, M.R., Rayner, P.J., 877  
Scholes, R.J., Steffen, W.L., Wirth, C., 2001. Recent patterns 878  
and mechanisms of carbon exchange by terrestrial ecosystems. 879  
*Nature* 414, 169–172. 880
- Sellers, P.J., Berry, J.A., Collatz, G.J., Field, C.B., Hall, F.G., 881  
1992. Canopy reflectance, photosynthesis and transpiration. 882  
Part III. A reanalysis using enzyme kinetics-electron transport 883  
models of leaf physiology. *Remote Sens. Environ.* 42, 187– 884  
216. 885
- Sellers, P.J., Randall, D.A., Collatz, G.J., Berry, J.A., Field, C.B., 886  
Dazlich, D.A., Zhang, C., Collello, G.D., Bounoua, L., 1996a. A 887  
revised land surface parameterization (SSiB<sub>2</sub>) for atmospheric 888  
GCMs. Part I. Model formulation. *J. Climate* 9, 676– 889  
705. 890
- Sellers, P.J., Bounoua, L., Collatz, G.J., Randal, D.A., Dazlich, 891  
D.A., Los, S.O., Berry, J.A., Fung, I., Tucker, C.J., Field, C.B., 892  
Jensen, T.G., 1996b. Comparison of radiative and physiological 893  
effects of doubled atmospheric CO<sub>2</sub> on climate. *Science* 271, 894  
1402–1406. 895
- Sellers, P.J., Dickinson, R.E., Randall, D.A., Betts, A.K., Hall, 896  
F.G., Berry, J.A., Collatz, G.J., Denning, A.S., Mooney, H.A., 897  
Nobre, C.A., Sato, N., Field, C.B., Henderson-Sellers, A., 1997. 898  
Modeling the exchanges of energy, water, and carbon between 899  
continents and the atmosphere. *Science* 275 (5299), 502–509. 900
- Shuttleworth, W.J., Gash, J.H.C., Roberts, J.M., Nobre, C.A., 901  
Molion, L.C.B., Ribeiro, M.N.G., 1991. Post-deforestation 902  
Amazonian climate: Anglo-Brazilian research to improve 903  
prediction. *J. Hydrol.* 129, 71–86. 904
- Thornley, J.H.M., Johnson, I.R., 1990. *Plant and Crop Modelling.* 905  
Oxford University Press, Oxford, 669 p. 906
- Tian, H., Melillo, J.M., Kicklighter, D.W., McGuire, A.D., 907  
Helfrich, J., Moore, B., Vorosmarty, C.J., 2000. Climatic 908  
and biotic controls on annual carbon storage in Amazonian 909  
ecosystems. *Global Ecol. Biogeography* 9, 315–335. 910
- Williams, M., Malhi, Y., Nobre, A.D., Rastetter, E.B., Grace, 911  
J., Pereira, M.G.P., 1998. Seasonal variation in net carbon 912  
exchange and evapotranspiration in a Brazilian rain forest: a 913  
modelling analysis. *Plant, Cell Environ.* 21, 953–968. 914
- Wright, I.R., Gash, J.H.C., Rocha, H.R., Shuttleworth, W.J., 915  
Nobre, C.A., Carvalho, P.R.A., Leitao, M.V.B.R., Maitelli, G.T., 916  
Zamponi, C.A.G.P., 1992. Dry season micrometeorology of 917  
Amazonian ranchland. *Quart. J. Roy. Meteor. Soc.* 118, 1083– 918  
1099. 919

- 920 Xue, Y., Sellers, P.J., Kinter III, J.L., Shukla, J., 1991. A simplified  
921 biosphere model for global climate studies. *J. Climate* 4, 345–  
922 364.
- 923 Xue, Y., Bastable, H.G., Dirmeyer, P.A., Sellers, P.J., 1996a.  
924 Sensitivity of simulated surface fluxes to changes in land  
925 surface parameterization—a study using ABRACOS data. *J.*  
926 *Appl. Meteor.* 35, 386–400.
- 927 Xue, Y., Zeng, F.J., Schlosser, C.A., 1996b. SSiB and its sensitivity  
928 to soil properties—a case study using HAPEX-Mobilhy data.  
929 *Global Planetary Change* 13, 183–194.
- Xue, Y., Sellers, P.J., Zeng, F.J., Schlosser, C.A., 1997. Com- 930  
ments on “Use of midlatitude soil moisture and meteorolo- 931  
gical observations to validate soil moisture simulations 932  
with biosphere and bucket models”. *J. Climate* 10, 374– 933  
376. 934
- Xue, Y., Zeng, F.J., Mitchell, K., Janjic, Z., Rogers, E., 2001. 935  
The impact of land surface processes on the simulation of 936  
the US hydrological cycle: a case study of US 1993 flood 937  
using the Eta/SSiB regional model. *Mon. Wea. Rev.* 129, 2833– 938  
2860. 939